

# A SEARCH FOR FRB 121102-LIKE PERSISTENT RADIO-LUMINOUS SOURCES – CANDIDATES AND IMPLICATIONS FOR THE FRB RATE AND SEARCHES

ERAN O. OFEK<sup>1</sup>

*Submitted to ApJ*

## ABSTRACT

The localization of the repeating fast radio burst (FRB), FRB 121102, suggests that it is associated with a persistent radio-luminous compact source in the FRB host galaxy. Using the FIRST radio catalog, I present a search for luminous persistent sources in nearby galaxies, with radio luminosities  $> 10\%$  of the FRB 121102 persistent source luminosity. The galaxy sample contains about 30% of the total galaxy  $g$ -band luminosity within  $< 108$  Mpc, in a footprint of  $10,600 \text{ deg}^2$ . After rejecting sources likely due to active galactic nuclei activity or background sources, I remain with 11 candidates that are presumably associated with galactic disks or star formation regions. At least some of these candidates are likely to be due to chance alignment. In addition, I find 85 sources within  $1''$  of galactic nuclei. Assuming the radio persistent sources are not related to galactic nuclei and that they follow the galaxy  $g$ -band light, the 11 sources imply a 95% confidence upper limit on the space density of luminous persistent sources of  $\lesssim 5 \times 10^{-5} \text{ Mpc}^{-3}$ , and that at any given time only a small fraction of galaxies host a radio luminous persistent source ( $\lesssim 10^{-3} L_{*}^{-1}$ ). Assuming persistent sources life time of 100 yr, this implies a birth rate of  $\lesssim 5 \times 10^{-7} \text{ yr}^{-1} \text{ Mpc}^{-3}$ . Given the FRB volumetric rate, and assuming that all FRBs repeat and are associated with persistent radio sources, this sets a lower limit on the rate of FRB events per persistent source of  $\gtrsim 0.8 \text{ yr}^{-1}$ . I argue that these 11 candidates are good targets for FRB searches and I estimate the FRB event rate from these candidates.

*Subject headings:* galaxies: general — galaxies: statistics

## 1. INTRODUCTION

Fast radio bursts are dispersed millisecond-duration pulses observed at GHz frequencies (Lorimer et al. 2007; Thornton et al. 2013). Spitler et al. (2016) reported the discovery of a repeating FRB, and follow-up observations using the Very Large Array (VLA) were able to provide an arcsecond localization of the source of the bursts (Chatterjee et al. 2017). The localization is consistent with the position of a star formation region in a faint galaxy ( $r = 25.1$  mag) at a redshift of 0.19273 (Tendulkar et al. 2017; Bassa et al. 2017). Furthermore, Chatterjee et al. (2017) reported the existence of a persistent radio source within  $1''$  of the FRB location, and Marcote et al. (2017) showed that the FRB and the persistent source are separated by less than 12 mas ( $\lesssim 40$  pc projected). The radio source has a mean flux density of about 0.18 mJy, it is variable, presumably due to scintillations, and unresolved with an angular size smaller than about 1.7 mas.

There are many suggestions for the FRB mechanism, including soft gamma-ray repeats (e.g., Popov & Postnov 2010; Kulkarni et al. 2014; Lyubarsky 2014; see however Tendulkar et al. 2016), Galactic stars (e.g., Maoz et al. 2015), pulsars (e.g., Lyutikov et al. 2016; Katz 2017a), magnetars (e.g., Metzger et al. 2017), pulsar wind nebulae (e.g., Dai, Wang & Yu 2017), active galactic nuclei (Katz 2017b), and more. Based on the FRB 121102 persistent source luminosity, spectrum, angular size, and the FRBs constant dispersion measure (DM) over a year time scale, Waxman (2017) inferred the properties of the emitting region. He concluded it is a mildly relativistic,  $10^{-5} M_{\odot}$  shell which propagates into an ambient medium. The energy of this expanding shell is of the order of  $10^{49}$  erg, and its lifetime is of order  $\lesssim 300$  yr. Waxman (2017) also sug-

gested an efficient mechanism that produces the FRBs within this persistent source via synchrotron maser.

An intriguing property of the FRB 121102 persistent source is that it is radio bright. With an isotropic radiative energy of  $\nu L_{\nu} \approx 3 \times 10^{38} \text{ erg s}^{-1}$ , at 1.4 GHz, it is over an order of magnitude brighter than the brightest known supernova (SN) remnants (e.g., Lonsdale et al. 2006; Parra et al. 2007; Chomiuk & Wilcots 2009). However, its luminosity is comparable with the brightest young ( $\sim 1$  yr old) SNe (e.g., Weiler et al. 2002).

Spitler et al. (2016) showed that the FRBs' arrival times are highly non Poissonic (see also e.g., Wang & Yu 2017). This fact makes it difficult to estimate the actual mean rate of the FRB 121102 events.

Here, I report on a search for persistent radio sources in galaxies in the nearby Universe ( $z < 0.025$ ). I find 11 candidates, with luminosity greater than 10% of the FRB 121102 persistent source. Regardless of the nature of these luminous radio sources, and their relation to FRBs, by estimating the completeness of the survey I was able to place an upper limit on the number density of such bright compact persistent sources in the local Universe. Furthermore, assuming that all the FRBs repeat and associated with persistent radio sources, I set a lower limit on the rate of FRB events per persistent source. I also discuss the volumetric rate of FRBs and the implications for FRB searches.

The structure of this paper is as follows: In §2 I describe the search for persistent sources in the nearby Universe, while in §3 I analyze the results. The nature of the persistent radio sources is discussed in §4, and in §5 I summarize the results and discuss the implications for FRB searches.

## 2. SEARCH FOR FRB PERSISTENT SOURCES

Here I present a search for persistent radio-luminous compact sources in the nearby Universe. In §2.1 I present the nearby galaxy sample, and in §2.2 I describe the cross match-

<sup>1</sup> Benozio Center for Astrophysics, Weizmann Institute of Science, 76100 Rehovot, Israel

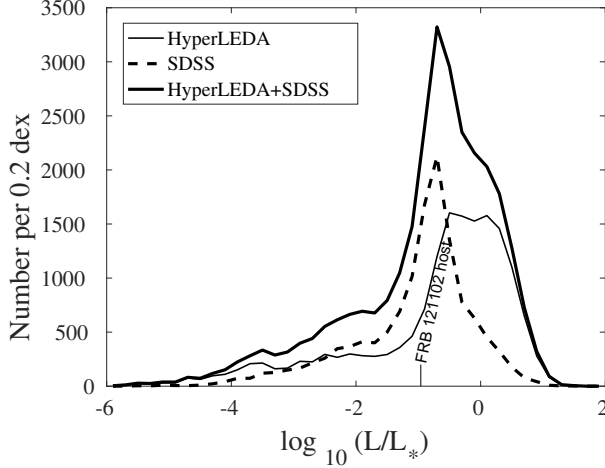


FIG. 1.— The luminosity function of the HyperLEDA (thin solid line), SDSS (dashed line), and combined catalog galaxies (thick solid line). The luminosity is presented in units of  $L_*$  which I here define to corresponds to  $g$ -band absolute magnitude of  $-19$ . All galaxy magnitude are SDSS  $g$ -band model magnitude. The Y-axis shows the number of galaxies per 0.2 logarithmic bins. The vertical line on the bottom indicates the approximate luminosity of the FRB 121102 host galaxy.

ing of the galaxy list with the FIRST radio catalog. In §2.3 I estimate chance coincidence probabilities, while in §2.4 I discuss the radio sources' variability. All the steps and analysis were performed using tools and catalogue available in the MATLAB Astronomy & Astrophysics Toolbox<sup>2</sup> (Ofek 2014).

### 2.1. The nearby galaxy sample and its completeness

I compiled a catalog of nearby galaxies within 108 Mpc. The catalog is based on combining the HyperLEDA galaxies<sup>3</sup> (Paturel et al. 2003; Makarov et al. 2014) with the NASA Extragalactic Database (NED<sup>4</sup>) redshifts, and the Sloan Digital Sky Survey (SDSS; York et al. 2000) galaxies with known redshifts. Both catalogs are restricted to the FIRST<sup>5</sup> radio survey footprint (Becker, White, & Helfand 1995). This catalog is far from being complete and I estimate its completeness below. I note that the total area of the FIRST footprint is about  $10,600 \text{ deg}^2$ .

The HyperLEDA catalog lists galaxies brighter than 18 mag, without redshifts. I compiled a catalog of all redshifts available in NED<sup>6</sup>. I cross-matched galaxies in the HyperLEDA catalog with the redshift catalog. The association radius was set to  $15''$ . Next, I selected only galaxies with redshifts in the range 0 to 0.025 that are found in the FIRST footprints. Specifically, I demand that the FIRST coverage maps at the galaxy position have rms below 0.26 mJy and above zero. The resulting catalog has 16,152 entries.

I supplemented this catalog with SDSS galaxies in the FIRST footprint<sup>7</sup>, with redshifts above 0 and below 0.025 that are not listed in the HyperLEDA catalog ( $5''$  association). This catalog contains an additional 12,663 galaxies. All the galaxies' magnitudes were corrected for Galactic extinction

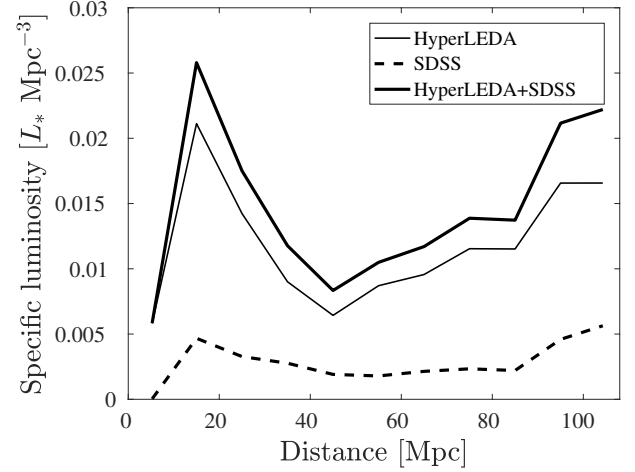


FIG. 2.— The luminosity density in the galaxy catalog as a function of distance (corrected for the FIRST footprint sky area).

(Cardelli et al. 1989; Schlegel et al. 1998).

The luminosity functions of the two galaxy catalogue are shown in Figure 1. The luminosity function shows a steep drop for galaxies fainter than about  $0.1 L_*$ . I note that the FRB 121102 host galaxy luminosity is near the peak of the luminosity function in Figure 1.

Next, I estimate the completeness of the combined galaxy catalog in terms of total  $g$ -band luminosity in the nearby Universe. Figure 2 shows the galaxy sample  $g$ -band luminosity per unit volume as a function of distance. I also integrated the total  $B$ -band luminosity in the Karachentsev et al. (2004) catalog of galaxies within 10 Mpc. In order to correct for the galaxy zone of avoidance, I restricted the search again to the FIRST footprints. Since the Karachentsev et al. catalog lists the  $B$ -band magnitude, while our catalog uses the SDSS  $g$ -band, I use a  $B(\text{Vega}) - g(AB) = 0.18 \text{ mag}$  correction<sup>8</sup>. I find that the  $g$ -band luminosity density in the Karachentsev et al. (2004) catalog is about  $0.055 L_* \text{ Mpc}^{-3}$ , where here  $L_*$  is the luminosity corresponding to  $g$ -band absolute magnitude of  $-19$ . This is close to the measured  $L_*$  at  $z = 0.1$  ( $\approx -18.8$ ; e.g., Montero-Dorta & Prada 2009).

Assuming that the Karachentsev et al. (2004) catalog is nearly complete in terms of the total luminosity and star formation rate<sup>9</sup>, and that the galaxy luminosity density within 10 Mpc is representative of the galaxy luminosity density at larger distances, I calculate how much luminosity is missing from our HyperLEDA+SDSS catalog per unit volume as a function of distance, and integrate. I find that the total luminosity in our catalog has a completeness of 30%. I note that this factor is uncertain due to the fact that the galaxy distribution is correlated. Given the galaxy correlation function (Tucker et al. 1997; Zehavi et al. 2002) I estimate the completeness to have about 10% uncertainty.

### 2.2. Search for radio sources associated with nearby galaxies

I cross-matched our galaxy catalogs with FIRST point sources. I defined point sources to have a major axis smaller

<sup>2</sup> <https://webhome.weizmann.ac.il/home/eofek/matlab/>

<sup>3</sup> <http://leda.univ-lyon1.fr/>

<sup>4</sup> <https://ned.ipac.caltech.edu/>

<sup>5</sup> FIRST catalog version 2017 Dec 14.

<sup>6</sup> This catalog, with  $3.27 \times 10^6$  redshifts, is available as part of the MATALB Astronomy & Astrophysics Toolbox (Ofek 2014), under `cats.galaxies.NED_z`.

<sup>7</sup> The SDSS catalog contains many HyperLEDA galaxies.

<sup>8</sup> Assuming a black-body spectrum with an effective temperature of 6000 K.

<sup>9</sup> If this assumption was wildly incorrect, then we would expect that blind SN surveys will find many more nearby SN associated with faint dwarf galaxies.

than 3 times the uncertainty<sup>10</sup> in the radio size measurement. The HyperLEDA-catalog search radius, for each galaxy, was set to the galaxy's 25 mag arcsec<sup>-2</sup> surface brightness semi-major axis listed in the catalog, while for the SDSS sample I used the SDSS Petrosian radius<sup>11</sup>.

In the cross-matching step, I selected only sources with intrinsic radio luminosity (assuming at the galaxy redshift) of  $> 10\%$  of the luminosity of the persistent source associated with FRB 121102. For this, I used the FRB 121102 persistent source mean radio flux density of 0.18 mJy and luminosity distance of 938 Mpc (i.e.,  $\nu L_\nu \approx 3 \times 10^{38} \text{ erg s}^{-1}$ ).

The cross-matching yielded 122 possible matches, of which 91 are from the HyperLEDA catalog and 31 are from the SDSS catalog. The candidates are listed in Table 1, and in §2.3 I discuss the chance coincidence probability for these sources.

I inspected the SDSS and WISE (Wright et al. 2010) 4.6 micron-band images of all candidates. The most common candidates are associated with galactic nuclei to within 1 arcsec (85 sources). In these cases I assumed that the radio source is due to active galactic nuclei (AGN) activity in the galaxy center. As most radio sources above a flux density of a few mJy are AGNs, this assumption is probably reasonable. I further note that at a redshift of 0.025 one arcsec corresponds to about 0.5 kpc, which is an order of magnitude smaller than the typical size of galaxies. This gives some confidence that even if we remove from our sample persistent sources which are spatially coincidence with their galaxy's center, the number of non-AGN sources missed is small.

Many other sources seem to be projected on a galaxy, but outside any star formation region or light associated with the galaxy – these sources are sometimes associated with an unresolved source (likely a background quasar). Finally, 11 sources were found to coincide with galactic disks light, or compact star forming galaxies (similar to FRB 121102; Bassa et al. 2017). I regard these 11 sources as the persistent-source candidates, and they are listed at the top part of Table 1. However, if FRBs are related to AGN activity (e.g., Katz 2017; Vieyro et al. 2017), then the number of candidates changes to 85. Figure 3 shows the SDSS images of the 11 candidate galaxies, with markers showing the radio source position and galaxy center.

### 2.3. Chance coincidence

Given the total sky area of galaxies in our catalogs ( $\approx 5.3 \text{ deg}^2$ ), it is likely that at least some of the candidates are due to chance coincidence of background high-redshift sources with nearby galaxies. Here, I estimate the probability that the sources I find are background sources, unrelated to the spatially associated low-redshift galaxy.

For each galaxy in the catalogs (HyperLEDA and SDSS) I calculate its area on the celestial sphere (given its radius). Furthermore, given the galaxy distance, I calculate the number density of sources on the sky that are compact radio sources with luminosity  $> 10\%$  of the FRB 121102 persistent radio-source luminosity. By multiplying the area of each galaxy by the corresponding surface density of radio sources and summing, I find that the expectancy value for the number of chance-coincidence background sources is 37.7. Excluding the 85 sources found within 1" from galactic nuclei, there

are 37 sources spatially associated with nearby galaxies (i.e.,  $= 122 - 85$ ). The 1" exclusion is small compared with the typical galaxy dimension and has a negligible effect on the expectancy value for chance coincidence.

Given that the expectancy is 37.7 and that the observed number is 37, it is likely that at least some of the 11 candidates are due to chance coincidence. Assuming that the selection process (e.g., association with galaxy light in images) selects the best candidates, than the probability that all the 11 candidates are associated with their galaxy (rather than background sources) is 2.9%. The probability that at most 5, 2, 1, 0 of the 11 candidates are associated with their galaxy is 20%, 40%, 43%, and 50%, respectively.

This analysis suggests that some, or even all, of the 11 candidates I found are background sources unrelated to the spatially associated galaxy. If follow-up observations will indicate that all 11 candidates are unrelated to FRBs this will improve the upper limit on the luminous radio source space density (see §3.1) by a factor of about 7.

I note that a reasonable follow-up prioritization of the 11 candidates in Table 1 is by the inverse galaxy size and association with star-forming regions. One reason is that smaller galaxies have lower probability for chance coincidence with background objects. In this respect, the most interesting candidate in the list is J141918+394036. This source has the highest luminosity of all candidates and it is associated with a small-area blue galaxy.

### 2.4. Source variability

I cross-matched the sources in Table 1 with the NVSS catalog (Condon et al. 1998) with a 15" match radius. The NVSS flux and error are listed in Table 1. I further calculated, and list in Table 1,

$$\chi_{\text{NVSS-FIRST}} = \frac{f_{\text{NVSS}} - f_{\text{FIRST}}}{\sqrt{\Delta f_{\text{NVSS}}^2 + \Delta f_{\text{FIRST}}^2 + (\epsilon_{\text{cos}} f_{\text{FIRST}})^2}}. \quad (1)$$

Here  $f_{\text{NVSS}}$  is the NVSS<sup>12</sup> peak-flux density,  $f_{\text{FIRST}}$  is the FIRST peak-flux density,  $\Delta f_{\text{NVSS}}$ , and  $\Delta f_{\text{FIRST}}$  are the NVSS and FIRST flux errors, respectively, and  $\epsilon_{\text{cos}}$  is a calibration error assumed to be 0.03 (Condon et al. 1998). I note that Ofek et al. (2011) measurements of a few calibration sources suggest that the VLA calibration error may be smaller. Furthermore, Ofek & Frail (2011) found that any systematic offset between the FIRST and NVSS fluxes is small compared with the typical flux errors.

The FIRST-NVSS variability search indicates that these sources are roughly constant. However, I cannot rule out small amplitude variability due to scintillation or some long term decrease or increase in flux.

## 3. ANALYSIS

### 3.1. Persistent source volumetric density

I found 11 persistent source candidates. This sets a 95% (1-sided) upper limit of 18.2 sources in the searched volume (Gehrels 1986). Assuming the persistent source density is proportional to the  $g$ -band luminosity, and given the sky area and completeness of the catalog (§2.1), this gives 95% confidence-level upper limit on the number density of lumi-

<sup>10</sup> The size uncertainty is calculated using the formula in: <http://sundog.stsci.edu/first/catalogs/readme.html>

<sup>11</sup> <http://skyserver.sdss.org/dr7/en/help/docs/algorithm.asp?key=mag-petro>

<sup>12</sup> The NVSS and FIRST measurements each give a weighted mean flux over several epochs.

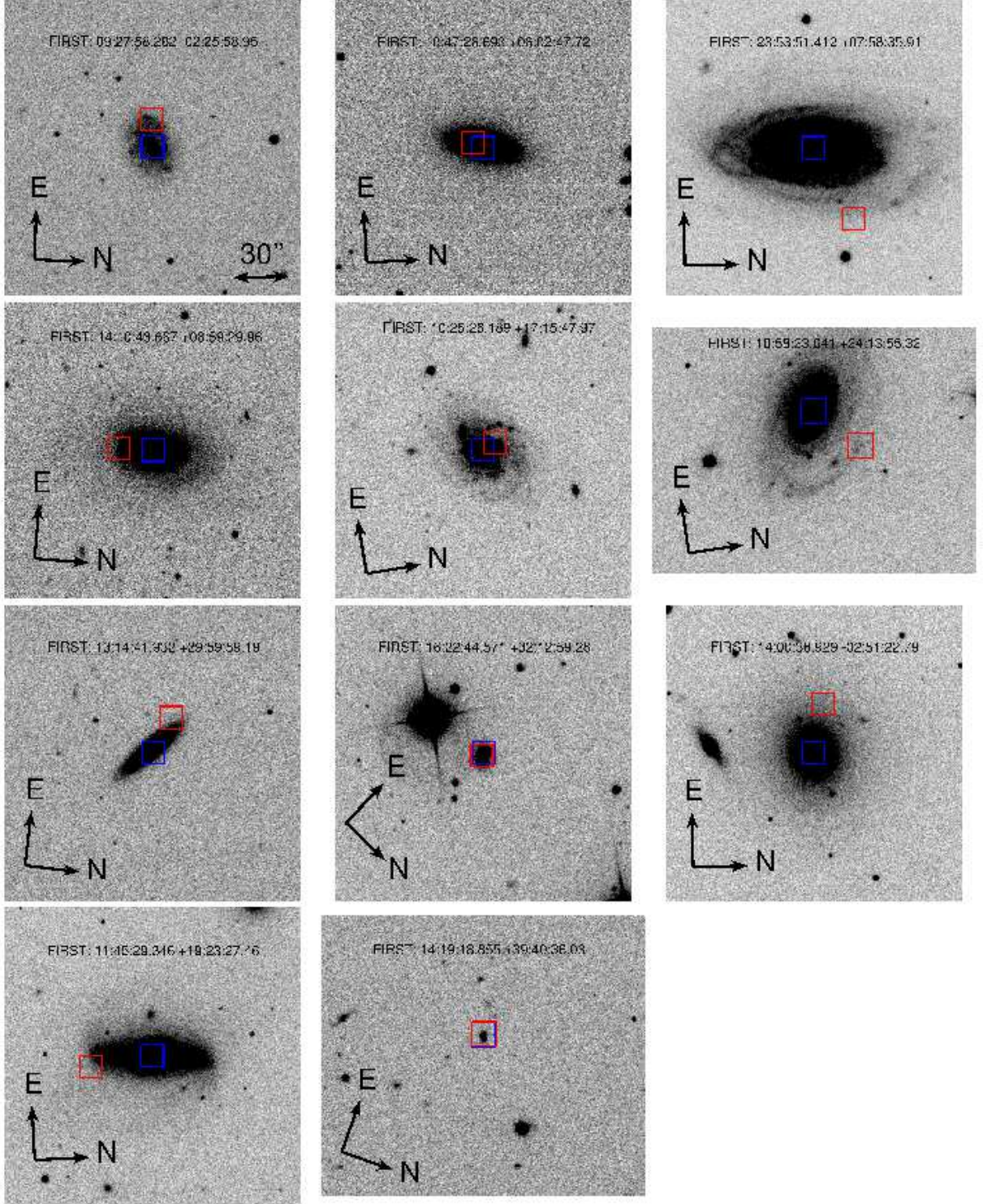


FIG. 3.— SDSS *g*-band images of the 11 luminous persistent source candidates. The blue boxes indicate the galaxies center while the red boxes show the radio sources position. See additional details in Table 1.

TABLE 1  
LUMINOUS PERSISTENT RADIO SOURCE CANDIDATES

| R.A.         | Dec.         | $f_p$<br>mJy | $\Delta f_p$<br>mJy | $L/L_{\text{pers}}$ | $z$   | $\theta$<br>arcsec | $f_{\text{NVSS}}$<br>mJy | $\Delta f_{\text{NVSS}}$<br>mJy | $\chi_{\text{NVSS-FIRST}}$ | $X_c$<br>ct/ks | Comment                                  |
|--------------|--------------|--------------|---------------------|---------------------|-------|--------------------|--------------------------|---------------------------------|----------------------------|----------------|--|
| 09:27:58.282 | -02:25:58.95 | 2.1          | 0.14                | 0.14                | 0.023 | 14.32              | ...                      | ...                             | ...                        | ...            | Spiral arm + IR source                   |
| 10:47:26.693 | +06:02:47.72 | 2.9          | 0.14                | 0.13                | 0.019 | 5.87               | 2.4                      | 0.4                             | -1.1                       | ...            | Off galaxy center; passive galaxy        |
| 23:53:51.412 | +07:58:35.91 | 4.2          | 0.13                | 0.16                | 0.018 | 42.68              | ...                      | ...                             | ...                        | ...            | Near spiral arm; near red+IR source      |
| 14:10:43.667 | +08:59:29.96 | 3.2          | 0.15                | 0.21                | 0.023 | 17.66              | 4.0                      | 0.4                             | 1.8                        | ...            | Edge of spiral disk; red faint source?   |
| 10:25:26.189 | +17:15:47.97 | 2.8          | 0.13                | 0.11                | 0.018 | 7.08               | ...                      | ...                             | ...                        | ...            | Spiral arm                               |
| 10:58:23.641 | +24:13:55.32 | 2.3          | 0.15                | 0.12                | 0.021 | 29.79              | ...                      | ...                             | ...                        | ...            | Spiral arm                               |
| 13:14:41.932 | +29:59:59.19 | 2.2          | 0.14                | 0.14                | 0.023 | 20.58              | 4.0                      | 0.5                             | 3.4                        | ...            | Edge of spiral galaxy; IR source         |
| 16:22:44.571 | +32:12:59.28 | 2.0          | 0.15                | 0.11                | 0.022 | 0.89               | 2.7                      | 0.4                             | 1.7                        | ...            | Small blue galaxy; near center           |
| 14:00:38.929 | -02:51:22.79 | 1.5          | 0.15                | 0.11                | 0.025 | 26.41              | ...                      | ...                             | ...                        | 18.8           | Elliptical galaxy halo; no vis/IR source |
| 11:45:29.346 | +19:23:27.46 | 3.5          | 0.20                | 0.26                | 0.025 | 33.35              | 2.4                      | 0.4                             | -2.3                       | ...            | Edge of galaxy; No optical or IR source  |
| 14:19:18.855 | +39:40:36.03 | 21.1         | 0.15                | 0.95                | 0.020 | 0.50               | 18.5                     | 1.0                             | -2.2                       | ...            | Compact blue star forming galaxy         |
| 00:17:27.498 | -09:34:26.56 | 2.5          | 0.15                | 0.15                | 0.023 | 0.51               | ...                      | ...                             | ...                        | ...            | Center of galaxy                         |
| 00:17:59.547 | -09:16:00.89 | 1.6          | 0.15                | 0.10                | 0.023 | 19.06              | 2.9                      | 0.5                             | 2.5                        | ...            | Halo of galaxy, likely IR source         |
| 02:52:42.189 | -08:48:15.76 | 3.1          | 0.15                | 0.12                | 0.018 | 0.18               | 4.4                      | 0.5                             | 2.4                        | ...            | Center of galaxy                         |
| 11:24:03.341 | -07:47:01.13 | 2.1          | 0.14                | 0.16                | 0.025 | 0.50               | 3.7                      | 0.6                             | 2.5                        | ...            | Center of galaxy                         |
| 01:44:43.099 | -04:07:46.25 | 5.2          | 0.13                | 0.21                | 0.018 | 34.81              | 10.9                     | 0.6                             | 9.0                        | ...            | Halo of galaxy, blue source + IR source  |

NOTE. — A list of radio sources that spatially coincide with nearby galaxies. Sources above the horizontal-line separator are the 11 candidates. The full table is available electronically, and here I present only the first several entries. R.A. and Dec. are the J2000.0 right ascension and declination, respectively, of the radio source,  $f_p$  is its peak radio flux,  $L/L_{\text{pers}}$  is its luminosity in units of the mean luminosity of the FRB 121102 persistence source,  $z$  is the spatially coincident galaxy redshift, and  $\theta$  is the angular separation between the galaxy and radio source.  $f_{\text{NVSS}}$  and  $\Delta f_{\text{NVSS}}$  are the NVSS flux density and its uncertainty, respectively,  $\chi_{\text{NVSS-FIRST}}$  is the FIRST to NVSS variability in units of the 1- $\sigma$  uncertainty (Equation 1), and  $X_c$  is the *ROSAT* counts per kilo-second, from the *ROSAT* bright and faint source catalogs (Voges et al. 1999; 2000). For the *ROSAT* catalogue, I used a 45'' search radius. Entries with no data indicate non detection.



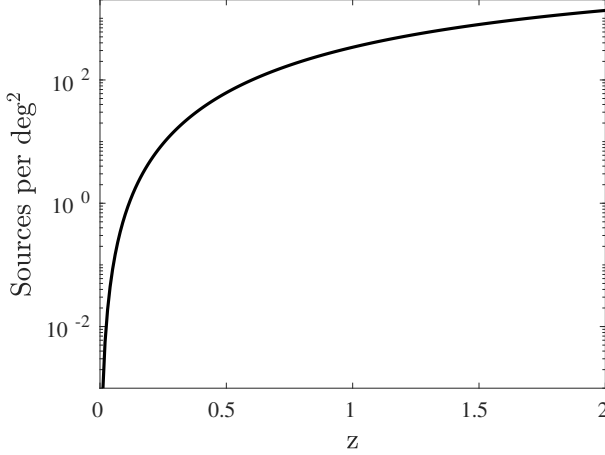


FIG. 4.— The upper limit on the sky surface density of radio luminous persistent sources up to a given redshift.

nous persistent sources of:

$$\rho_{pers} \lesssim 5 \times 10^{-5} \text{ Mpc}^{-3}. \quad (2)$$

Using the total galaxy luminosity per unit volume I found in §2.1, this is equivalent to a number of persistent sources per  $L_*$  galaxy of  $\lesssim 10^{-3} L_*^{-1}$ . However, if FRBs are related to galactic nuclei, then I find 85 candidates and the limit in Equation 2 will change to  $\lesssim 3 \times 10^{-4} \text{ Mpc}^{-3}$  ( $\lesssim 5 \times 10^{-3} L_*^{-1}$ ). I note that this estimate ignores any possible evolution of persistent sources with redshift. However, the expected increase in the star formation rate between  $z = 0$  to  $z = 0.025$  is only 8% (e.g., Wyder et al. 2005; Schiminovich et al. 2005). Given the density in Equation 2, Figure 4 presents the upper limit on the sky surface density of radio luminous persistent sources, as a function of redshift.

It is not yet clear whether the assumption that FRBs follow the galaxy light is correct. For example, based on the low luminosity of the FRB 121102 host (extinction corrected  $r$ -band abs. mag.  $-16.8$ ), Nicholl et al. (2017) claimed that FRBs prefer dwarf galaxies. Using the Karachentsev et al. (2004) catalog, I calculate the fraction of  $B$ -band luminosity in galaxies fainter than the host galaxy of FRB 121102 (i.e.,  $g$ -band abs. mag.  $-16.6$ ; assuming  $g - r \approx 0.2$  mag). I find that  $\approx 3\%$  of the luminosity is in galaxies fainter than abs. mag.  $-16.6$ . Since it is expected that there is some incompleteness even in the Karachentsev et al. catalog, the actual fraction can be a little bit higher. Therefore, I cannot rule out the possibility that the FRB 121102 host galaxy luminosity follows the general galaxy luminosity function, at more than 97% confidence.

I note that the luminosity of the FRB 121102 host galaxy is near the peak of the luminosity function of galaxies in my catalog. Therefore, even if the assumption that persistent radio sources follow the  $g$ -band light is incorrect, then my upper limit on the space density of radio persistent sources is likely still valid to an order of magnitude.

The upper limit on the FRB 121102 persistent source age estimated by Waxman (2017; see also Nicholl et al. 2017) is 300 yr, while the lower limit on its age is  $\gtrsim 5$  yr (Metzger et al. 2017; Waxman 2017). Adopting the persistent source age of  $\tau_{pers} \approx 100$  yr, our number density implies a birth rate of

$$\dot{\rho}_{pers, birthrate} \lesssim 5 \times 10^{-7} \left( \frac{\tau_{age}}{100 \text{ yr}} \right)^{-1} \text{ yr}^{-1} \text{ Mpc}^{-3}. \quad (3)$$

This suggests that the origin of FRB persistent sources is some sort of rare phenomenon (e.g., explosions). It is tempting to relate this birth rate to that of known events (e.g., Super Luminous Supernovae [SLSN] or Gamma-Ray Bursts [GRB]; e.g., Nicholl et al. 2017). However, SLSN and GRB can be seen to large distances, and it is very likely that other fainter, yet unknown, transient classes exist. In this context I note that Waxman (2017) found that the total energy of the nebula associated with the FRB 121102 persistent source is of the order of  $10^{49}$  erg. This is low relative to the energetics of *known* rare events.

### 3.2. The rate of FRBs

In order to constrain the rate of FRB events per persistent source, we need an estimate of the FRBs rate. There are many FRB rate estimates (e.g., Deneva et al. 2009; Burke-Spolaor et al. 2014; Champion et al. 2016; Lawrence et al. 2016; Vander Wiel et al. 2016). They are typically reported for different parameters (e.g., fluence limit and FRB duration), and therefore a comparison between these rates requires caution.

Furthermore, I note that FRB searches may be slightly biased by several reasons. For example: (1) Usually FRB searches are done up to some limiting dispersion measure (DM). The DM threshold may evolve with time (e.g., whenever a new record in DM is found, the DM threshold is updated). This may result in an incompleteness for bright/far FRB events. (2) FRB searches are performed using non-coherent de-dispersion. This may bias against FRBs with durations shorter than a fraction of a millisecond. I note that in Zackay & Ofek (2016) we suggested a computationally efficient method for calculating the coherent de-dispersion.

In order to avoid some of these complications, I prefer an estimate based on a single instrument. Therefore, for the rate estimate I adopt the Champion et al. (2016) analysis of ten FRBs detected by the Parkes telescope. Champion et al. (2016) report an FRB all-sky rate of  $R(F > 0.13 \text{ mJy ms}) = 7000^{+5000}_{-3000} \text{ day}^{-1}$  (95% confidence errors) above fluence of  $0.13 \text{ Jy ms}$  for a minimal  $0.128 \text{ ms}$  pulse duration.

I note that since the radio telescope beam is not uniform and the observed cumulative flux density function of sources (so called  $\log(N)$ - $\log(S)$ ) is some power-law ( $-3/2$  for Euclidean Universe; see however Vedantham et al. 2016), this may affect the effective beam size of the survey (used in the rate calculation). Assuming a cumulative flux density power-law of  $-3/2$  and assuming a Gaussian beam with a size equal to the beam full-width half maximum, the correction factor is 1 (see appendix C in Ofek et al. 2011). Therefore, here I adopt the Champion et al. (2016) rate.

### 3.3. The FRB volumetric rate

Assuming that all FRBs repeat, that they are associated with radio persistent sources, their emission is isotropic, and using the FRB rate (§3.2), I use the upper limit on the persistent source number density (Eq. 2) to put a lower limit on the rate of FRB events per persistent source.

The first step is to estimate the volumetric rate of FRBs. To estimate the effective volume of the Parkes search, I use all the 16 FRBs found by the Parkes radio telescope<sup>13</sup>. For each FRB DM I removed the estimated Milky Way DM, and I attributed

<sup>13</sup> Adopted from the FRB catalog: <http://www.astronomy.swin.edu.au/pulsar/frbcat/>

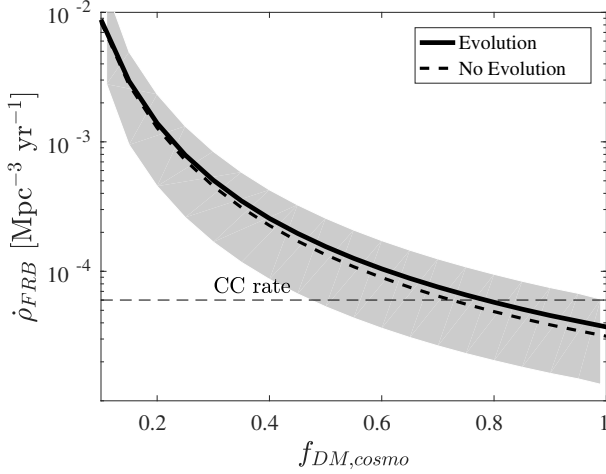


FIG. 5.— The estimated FRB rate per  $\text{Mpc}^{-3}$  as a function of  $f_{\text{DM,cosmo}}$ . The solid line shows the approximate FRB rate density assuming they follow the star formation rate, while the dashed line is assuming no evolution. The gray region indicates the approximate 68% confidence region, while the dashed horizontal line shows the core collapse SN rate (e.g., Li et al. 2011).

a fraction<sup>14</sup>  $f_{\text{DM,cosmo}}$  of the remaining DM to intergalactic dispersion. The analysis is performed for  $f_{\text{DM,cosmo}}$  in the range of 0.1 to 1. I converted the remaining intergalactic DM to redshift via the formulae in Zheng et al. (2014) assuming Planck cosmological parameters (Ade et al. 2015). Each redshift was transformed to a cosmological volume. Given a flux limited survey, Euclidian universe, and no cosmological evolution, the expectation value of the survey volume is two times the average of the volumes enclosed by the sources (e.g., similar to the argument of the  $V/V_{\text{max}}$  test; e.g., Schmidt 1968). Given the Universe geometry and cosmological evolution in the star formation rate, the ratio between the effective survey volume and the mean volume (corresponding to the redshift) of sources is somewhat smaller than 2 (i.e., star formation increases with redshift). In the calculation I assume the FRB rate follows the star formation rate and take into account the star-formation evolution from the compilation based on<sup>15</sup> Wyder et al. (2005), Schiminovich et al. (2005), Robotham & Driver (2011), and Cucciati et al. (2012). In any case, the effect of evolution is considerably smaller than the uncertainty in the rate estimate. This allows us to calculate the FRB volumetric rate as a function of  $f_{\text{DM,cosmo}}$ . Figure 5 shows the FRB rate as a function of  $f_{\text{DM,cosmo}}$ . Regardless of  $f_{\text{DM,cosmo}}$ , and assuming cosmological evolution in the FRB rate that follows the star formation rate, I find an FRB volumetric rate of

$$\dot{\rho}_{\text{FRB}} \gtrsim (3.7 \pm 2.4) \times 10^{-5} \text{Mpc}^{-3} \text{yr}^{-1}. \quad (4)$$

This estimate takes into account the effect of cosmological time dilation by multiplying the observed rate by  $(1 + \langle z \rangle)$ , where  $\langle z \rangle$  is the volume-weighted mean redshift of the FRBs. I note that this estimate depends on the unknown luminosity function of FRBs and should be regarded as an order of magnitude estimate. Furthermore, if the FRB emission is beamed then the rate at Equation 4 is, again, only a lower limit.

### 3.4. FRB rate per persistent source

<sup>14</sup> Attributing a fraction of the DM to intergalactic dispersion is an approximation – in practice the host galaxy DM is coming from some unknown probability distribution of host-galaxy DM.

<sup>15</sup> <https://ned.ipac.caltech.edu/level5/March14/Madau/Madau5.html>

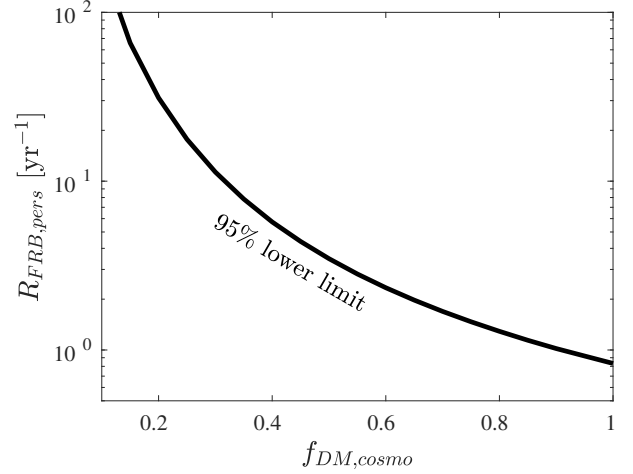


FIG. 6.— Lower limit on the FRB rate per persistent source as a function of  $f_{\text{DM,cosmo}}$ , as derived from the upper limit on the FRB persistent sources number density and the FRB volumetric rate. This lower limit on the rate corresponds to FRB events for which the intrinsic luminosity is as high as the FRBs seen by the Parkes telescope.

Assuming there is a steady state of FRB persistent source density that follows the star formation rate, and assuming that all FRBs are associated with persistent sources, I divide the lower limit on the FRB rate per unit volume (Eq. 4) by the upper limit on the persistent sources space density to derive a lower limit on the rate of FRBs per persistent source. Figure 6 presents the 95% confidence lower limit on rate of FRB events per persistent source as a function of  $f_{\text{DM,cosmo}}$ . For  $f_{\text{DM,cosmo}} = 1$  I find an FRB rate per persistent source of  $R_{\text{FRB,pers}} \gtrsim 0.8 \text{yr}^{-1}$ . This lower limit on the rate corresponds to FRB events for which the intrinsic luminosity is as high as the FRBs seen by Parkes.

### 3.5. Predictions and implications for observing strategy

An interesting implication is that if all FRBs repeat and are associated with luminous radio sources, then searches for FRBs in nearby galaxies (e.g., M31) using small radio dishes are likely to fail as on average only one in  $\gtrsim 1000$  galaxies hosts a luminous radio source. An observing strategy that is favored by my findings is to monitor for FRBs among the 11 candidates listed in Table 1. Figure 7 shows the predicted mean number of FRB events per persistent source per day that may be detected using a Parkes-like telescope if directed to an FRB-emitter source (i.e., presumably a persistent radio source) at a distance of 108 Mpc. This plot is shown for an FRB cumulative luminosity function  $\propto L^{-2/3}$ ,  $L^{-1}$ , and  $L^{-5/3}$ . The FRB rate per such source is estimated by

$$R_{\text{Parkes,108 Mpc}} \gtrsim R_{\text{FRB,pers}} \left( \frac{\langle d_{\text{Parkes}} \rangle}{108 \text{Mpc}} \right)^{-2\gamma}. \quad (5)$$

Here  $R_{\text{FRB,pers}}$  is the lower limit on the FRB rate per persistent source (§3.4; Fig. 6),  $\langle d_{\text{Parkes}} \rangle$  is the mean distance of the Parkes detected FRBs (§3.3; i.e.,  $z \approx 0.7$  for  $f_{\text{DM,cosmo}} = 1$ ), and  $\gamma$  is the assumed power-law index of the FRB cumulative luminosity function. I note that if FRBs emission is beamed in a constant direction then Figure 7 is correct on average for a population. However, in this case, some persistent radio sources will show no FRB emission. Furthermore, it is important to note that since the FRB 121102 events are not generated by a Poisson process, large deviations from the average expected rate are possible.

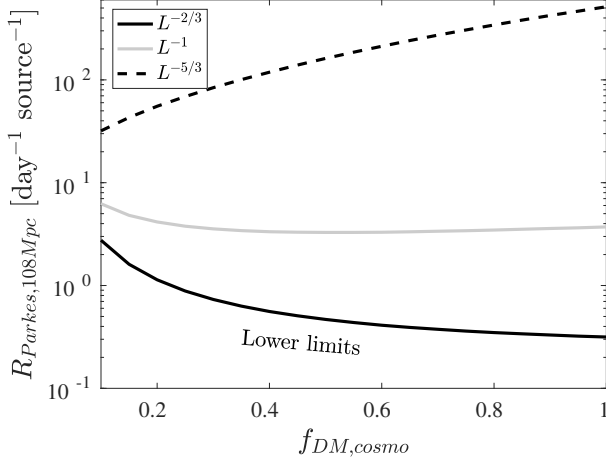


FIG. 7.— The predicted mean number of FRB events per day per persistent source detectable using a Parkes-like telescope, if directed to an FRB-emitter source (i.e., presumably a persistent radio source) at distance of 108 Mpc. This plot is shown for FRB cumulative luminosity function  $\propto L^{-2/3}$  (solid line),  $L^{-1}$  (gray line), and  $L^{-5/3}$  (dashed line). I note that the observed cumulative luminosity function of FRB 121102 is consistent with  $\propto L^{-2/3}$  (e.g., Nicholl et al. 2017).

#### 4. THE NATURE OF THE LUMINOUS RADIO SOURCES IN NEARBY GALAXIES

An intriguing question is what is the origin of the luminous radio sources reported here? It is likely that at least some of these sources are background objects unrelated to a nearby galaxy. Better estimate of the fraction of background objects requires follow-up observations. However, assuming that at least some of these sources are related to their spatially coincident galaxy, there are still several physical explanations.

First, it is possible that these sources are similar in nature to the radio persistent source associated with FRB 121102. This possibility can be further tested using follow-up radio spectral, temporal and interferometric observations.

Second, I would like to consider the possibility that some of these sources are just the bright end of the supernova (SN) remnants (SNR) luminosity function, or young SN with considerable circumstellar material that convert their kinetic energy to radiation on short time scales ( $\sim 1$  yr). This hypothesis can be tested by long-term monitoring of the radio sources, and a search for flux variability. I note that the brightest known radio SNe (e.g., Weiler et al. 2002) are as bright as the FRB 121102 persistent radio source. However, these SNe are variable on time scales of about one year, which is not consistent with the non-detection of variability between the NVSS (when available) and FIRST epochs which are typically several years apart.

Another possibility is gamma ray bursts (GRBs). In GRBs the ejecta velocity is much higher and therefore can produce luminous events (e.g., Levinson et al. 2002). In fact, in the past, the non-detection of transient radio sources was used to set an upper limit on the GRB space density, which can be translated to a lower limit on the GRBs beaming factor (Levinson et al. 2002; Gal-Yam et al. 2006).

Levinson et al. (2002) estimated the number of GRB radio afterglows in a flux-limited survey. However, our survey is both volume limited and luminosity limited. Therefore an upper limit on the number of expected GRB afterglows in our

survey is given by their rate in a volume limited survey

$$R_{GRB} \lesssim 0.2 \left( \frac{d}{108 \text{ Mpc}} \right)^3 \left( \frac{f_b}{1/75} \right)^{-1} \frac{\dot{\rho}_{GRB}}{0.5 \text{ Gpc}^{-3} \text{ yr}^{-1}} \text{ yr}^{-1}. \quad (6)$$

Here  $f_b$  is the GRB beaming factor (e.g., Gueta, Piran & Waxman 2005), and  $\dot{\rho}_{GRB}$  is their rate per unit volume. Assuming GRB afterglows can be observed for 100 yr (afterwards their luminosity is equivalent to that of SN remnants), and given the survey completeness, I conclude that there are  $\lesssim 1.5$  GRB afterglows in my sample.

In any case, there are two differences between GRB afterglows and the FRB persistent sources: The first is that while the FRB persistent sources are presumably expanding only mildly relativistically (Waxman 2017), GRB afterglows are expected to expand relativistically. This may result in some differences in the angular size of FRB persistent sources vs. GRB radio afterglows and the scintillation induced variability (e.g., different frequency-dependent variability). Furthermore, there may be some differences in the radio spectrum. I suggest that radio follow-up observations are required in order to reveal the nature of the luminous radio sources reported in this paper.

#### 5. SUMMARY

To summarize, I present a survey aimed at searching for luminous compact radio sources in galaxies with  $z < 0.025$ .

1. I find 11 sources with radio luminosity, at 1.4 GHz, of  $\nu L_\nu > 3 \times 10^{37} \text{ erg s}^{-1}$  (i.e.,  $> 10\%$  of the FRB 121102 persistent source luminosity) which are spatially associated with disks or star-forming regions of galaxies. Here I exclude sources that are spatially coincidence with galactic centers.
2. Given the completeness estimate for the galaxy catalog, and the FIRST survey area, I place an upper limit on the density of luminous persistent sources in the nearby Universe ( $\lesssim 5 \times 10^{-5} \text{ Mpc}^{-3}$ ). This upper limit assumes that luminous persistent sources follow the  $g$ -band luminosity of galaxies. If FRBs are related to galactic nuclei this limit will be changed to  $\lesssim 3 \times 10^{-4} \text{ Mpc}^{-3}$ .
3. Such luminous radio sources are rare – about  $\lesssim 10^{-3}$  per  $L_*$  galaxy.
4. Assuming a persistent source life time of  $t_{\text{age}} = 100 \text{ yr}$ , their birth rate is  $\lesssim 5 \times 10^{-7} (t_{\text{age}}/100 \text{ yr})^{-1} \text{ yr}^{-1} \text{ Mpc}^{-3}$ .
5. Assuming all FRBs repeat and are associated with persistent radio sources, I set a lower limit on the FRB rate per persistent source of  $\gtrsim 0.8 \text{ yr}^{-1}$ .
6. About 3% of the galaxy-population integrated luminosity is in galaxies fainter than the absolute mag. of the FRB 121102 host ( $g \approx -16.6$ ). This suggests that it is too early to conclude that FRBs prefer dwarf galaxies.
7. If some of the candidates in Table 1 are associated with FRBs then a few-days observation with sensitive (i.e., Parkes-like) radio telescopes may reveal FRB events from these sources. The detection of FRBs from such nearby galaxies may allow us to resolve the persistent



source, and to probe the FRB luminosity function at lower luminosities than in the case of FRB 121102.

I would like to thank Eli Waxman, Doron Kushnir, and Boaz Katz for the many discussions that led to this paper, and Orly Gnat, Barak Zackay, Eli Waxman, and Laura Spitler

for comments on the manuscript. I would also like to thank an anonymous referee for constructive comments. E.O.O. is grateful for support by grants from the Israel Science Foundation, Minerva, Israeli ministry of Science, the US-Israel Binational Science Foundation and the I-CORE Program of the Planning and Budgeting Committee and The Israel Science Foundation.

#### REFERENCES

- Planck Collaboration, Ade, P. A. R., Aghanim, N., et al. 2015, *A&A*, 580, A22
- Bassa, C. G., Tendulkar, S. P., Adams, E. A. K., et al. 2017, arXiv:1705.07698
- Becker, R. H., White, R. L., & Helfand, D. J. 1995, *ApJ*, 450, 559
- Cardelli, J. A., Clayton, G. C., & Mathis, J. S. 1989, *ApJ*, 345, 245
- Champion, D. J., Petroff, E., Kramer, M., et al. 2016, *MNRAS*, 460, L30
- Chatterjee, S., Law, C. J., Wharton, R. S., et al. 2017, *Nature*, 541, 58
- Chomiuk, L., & Wilcots, E. M. 2009, *ApJ*, 703, 370
- Cucciati, O., Tresse, L., Ilbert, O., et al. 2012, *A&A*, 539, A31
- Dai, Z. G., Wang, J. S., & Yu, Y. W. 2017, *ApJ*, 838, L7
- Gehrels, N. 1986, *ApJ*, 303, 336
- Guetta, D., Piran, T., & Waxman, E. 2005, *ApJ*, 619, 412
- Karachentsev, I. D., Karachentseva, V. E., Huchtmeier, W. K., & Makarov, D. I. 2004, *AJ*, 127, 2031
- Katz, J. I. 2017a, arXiv:1704.08301
- Katz, J. I. 2017b, arXiv:1702.02161
- Kulkarni, S. R., Ofek, E. O., Neill, J. D., Zheng, Z., & Juric, M. 2014, *ApJ*, 797, 70
- Lawrence, E., Vander Wiel, S., Law, C. J., Burke Spolaor, S., & Bower, G. C. 2016, arXiv:1611.00458
- Levinson, A., Ofek, E. O., Waxman, E., & Gal-Yam, A. 2002, *ApJ*, 576, 923
- Li, W., Chornock, R., Leaman, J., et al. 2011, *MNRAS*, 412, 1473
- Lonsdale, C. J., Diamond, P. J., Thrall, H., Smith, H. E., & Lonsdale, C. J. 2006, *ApJ*, 647, 185
- Lorimer, D. R., Bailes, M., McLaughlin, M. A., Narkevic, D. J., & Crawford, F. 2007, *Science*, 318, 777
- Lyubarsky, Y. 2014, *MNRAS*, 442, L9
- Lyutikov, M., Burzawa, L., & Popov, S. B. 2016, *MNRAS*, 462, 941
- Maoz, D., Loeb, A., Shvartzvald, Y., et al. 2015, *MNRAS*, 454, 2183
- Makarov D., Prugniel P., Terekhova N., Courtois H., & Vauglin I. 2014, *A&A*, 570, A13
- Marcote, B., Paragi, Z., Hessels, J. W. T., et al. 2017, *ApJ*, 834, L8
- Metzger, B. D., Berger, E., & Margalit, B. 2017, arXiv:1701.02370
- Montero-Dorta, A. D., & Prada, F. 2009, *MNRAS*, 399, 1106
- Nicholl, M., Williams, P. K. G., Berger, E., et al. 2017, arXiv:1704.00022
- Ofek, E. O., & Frail, D. A. 2011, *ApJ*, 737, 45
- Ofek, E. O., Frail, D. A., Breslau, B., et al. 2011, *ApJ*, 740, 65
- Ofek, E. O. 2014, *Astrophysics Source Code Library*, ascl:1407.005
- Parra, R., Conway, J. E., Diamond, P. J., et al. 2007, *ApJ*, 659, 314
- Popov, S. B., & Postnov, K. A. 2010, *Evolution of Cosmic Objects through their Physical Activity*, 129
- Robotham, A. S. G., & Driver, S. P. 2011, *MNRAS*, 413, 2570
- Schiminovich, D., Ilbert, O., Arnouts, S., et al. 2005, *ApJ*, 619, L47
- Schlegel, D. J., Finkbeiner, D. P., & Davis, M. 1998, *ApJ*, 500, 525
- Schmidt, M. 1968, *ApJ*, 151, 393
- Spitler, L. G., Scholz, P., Hessels, J. W. T., et al. 2016, *Nature*, 531, 202
- Tendulkar, S. P., Kaspi, V. M., & Patel, C. 2016, *ApJ*, 827, 59
- Tendulkar, S. P., Bassa, C. G., Cordes, J. M., et al. 2017, *ApJ*, 834, L7
- Thornton, D., Stappers, B., Bailes, M., et al. 2013, *Science*, 341, 53
- Vedantham, H. K., Ravi, V., Hallinan, G., & Shannon, R. M. 2016, *ApJ*, 830, 75
- Vieyro, F. L., Romero, G. E., Bosch-Ramon, V., Marcote, B., & del Valle, M. V. 2017, arXiv:1704.08097
- Voges, W., Aschenbach, B., Boller, T., et al. 1999, *A&A*, 349, 389
- Voges, W., Aschenbach, B., Boller, T., et al. 2000, *IAU Circ.*, 7432, 1
- Wang, F. Y., & Yu, H. 2017, *JCap*, 3, 023
- Waxman, E. 2017, arXiv:1703.06723
- Weiler, K. W., Panagia, N., Montes, M. J., & Sramek, R. A. 2002, *ARA&A*, 40, 387
- Wright, E. L., Eisenhardt, P. R. M., Mainzer, A. K., et al. 2010, *AJ*, 140, 1868-1881
- Wyder, T. K., Treyer, M. A., Milliard, B., et al. 2005, *ApJ*, 619, L15
- York, D. G., Adelman, J., Anderson, J. E., Jr., et al. 2000, *AJ*, 120, 1579
- Zehavi, I., Blanton, M. R., Frieman, J. A., et al. 2002, *ApJ*, 571, 172
- Zheng, Z., Ofek, E. O., Kulkarni, S. R., Neill, J. D., & Juric, M. 2014, *ApJ*, 797, 71